ISBN: 978-3-95450-241-7 ISSN: 2673-5350 doi:10.18429/JACoW-IBIC2022-WEP10

DETECTION OF A DC ELECTRIC FIELD USING ELECTRO-OPTICAL CRYSTALS

A. Cristiano*[1], M. Krupa, CERN, Geneva, Switzerland
R. Hill, University of Huddersfield, UK
[1]also at University of Huddersfield, UK

Abstract

Standard Beam Position Monitors (BPM) are intrinsically insensitive to beams with no temporal structure, so-called DC beams, which many CERN experiments rely on. We therefore propose a novel detection technique in which the usual BPM electrodes are replaced with electro-optic (EO) crystals. When exposed to an electric field, such crystals change their optical properties. This can be exploited to encode the electric field magnitude onto the polarisation state of a laser beam crossing the crystal. An additional EO crystal, placed outside the vacuum chamber, can be used to control the system's working point and to introduce a sinusoidal modulation, allowing DC measurements to be performed in the frequency domain. This contribution presents the working principle of this measurement technique, its known limitations, and possible solutions to further increase the system's performance. Analytical results and simulations for a double-crystal optical chain are benchmarked against the experimental data taken on a laboratory test bench.

INTRODUCTION

Most high-energy particle accelerators rely on radiofrequency cavities to boost bunches of particles to the desired energy. The power spectral density of such beams extends to high frequencies. However, some physics experiments require particle beams without any temporal structure [1], e.g. the future Search for Hidden Particle (SHiP) experiment at CERN [2]. Since DC particle beams do not induce signals in commonly used Beam Position Monitors, other methods are used to observe their transverse position. Indirect measurements can be performed with Schottky monitors [3], but they require some integration time. On the other hand, screen-based BPMs [4] interact with the particle beam and unavoidably affect its parameters which can deteriorate the beam. To address these issues, a novel BPM based on electro-optical crystals and suitable for measurement of DC beams (EO-DC-BPM) is under development at CERN.

Under an electric field exposure, EO crystals' properties change linearly due to the Pockels effect [5]. This variation can be encoded into the polarisation state of a laser beam crossing the crystal and later decoded through interferometric or amplitude demodulation techniques. The fast response of the Pockels effect makes EO crystals suitable for high frequency diagnostic tools. A high-frequency EO BPM capable of detecting variations of the transverse position within a bunch of a particle beam is currently under development for the HL-LHC project [6]. However, EO crystals are dielectric and in a presence of a DC or quasi-DC electromagnetic field, free charge carriers move to their boundaries and create an internal electric field obstructing the external field. This reduction of the modulation depth leads to a measurement error and has limited the use of EO materials to measurements above 20 Hz [7], unless the space charge is avoided through mechanical rotary stages [8].

Until now, the EO-DC-BPM development has focused on studying the feasibility of using an optical chain based on EO-crystals for measurements of the intensity of an electrostatic field in frequency domain. A proof-of-concept test bench has been designed to scrutinize the experimentally obtained results against those expected from simulations.

ELECTRO-OPTIC DC FIELD SENSOR

The EO-DC-BPM consists of four identical optical branches arranged symmetrically around the vacuum chamber. Each branch accommodates a chain of two electro-optical crystals. One crystal is placed inside the vacuum chamber and couples to the electrostatic field of the particle beam. The other crystal remains outside and is externally modulated with a sinusoidal field to move the measurement to the frequency domain. On top of the modulation signal, a DC bias is used to tune the system and to compensate crystal drifts which can lead to measurement error.

A conceptual overview of a single optical branch of the EO-DC-BPM is shown in Fig. 1. The sensor is composed of two EO crystals made of Lithium Niobate ($LiNbO_3$) which was chosen due to its large EO coefficients, low conductivity [9] and high radiation hardness [10] compared to other EO materials. The optical axes of the crystals are aligned with the z-axis. A linearly polarised laser beam traverses the crystals along the y-axis and oscillates in x-z plane.

The input polariser fixes the laser beam's polarisation at 45° with respect to the x-axis. The laser beam then enters

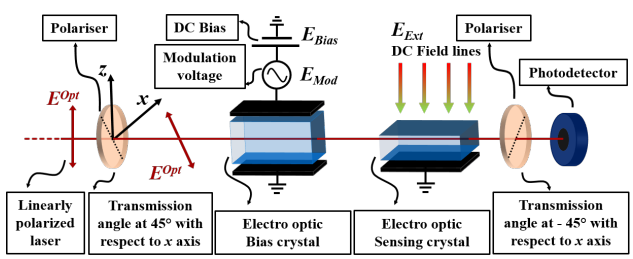

Figure 1: Schematic view of one optical branch of the EO-DC-BPM.

* antonio.cristiano@cern.ch

Content from this work may be used under the terms of the CC BY 4.0 licence (© 2022). Any distribution of this work must maintain attribution to the author(s), title of the work, publisher, and DOI

ISBN: 978-3-95450-241-7 ISSN: 2673-5350 doi:10.18429/JACoW-IBIC2022-WEP10

Content from this work may be used under the terms of the CC BY 4.0 licence (© 2022). Any distribution of this work must maintain attribution to the author(s), title of the work, publisher, and DOI

the first crystal, labelled as *EO Bias crystal* in Fig. 1. The phases of the two light components along the x-axis and z-axis are unevenly retarded because of the crystal's natural birefringency and the Pockels effect due to the external modulation field. The laser beam's polarisation is rotated again in the second crystal, *EO Sensing crystal*, in which the Pockels effect is driven by the external DC field to sense. Finally, the output polariser, rotated by 90° with respect to the first one, translates the polarisation modulation into optical power variation which can be measured by a photo-detector.

The optical chain has been modeled analytically [11] using Jones calculus [12]. The normalized output laser beam intensity is given by:

$$I = \sin^2[\alpha \cdot E_{Mod}(t) + \Gamma_0 + \Phi_0(E_{Bias}) + \Phi_1(E_{Ext})] \quad (1)$$

where $E_{Mod}(t)$ is the external sinusoidal modulation field, α is a constant term given by the physical and electro-optic properties of the bias crystal, Γ_0 is the collective phase retardation due to the natural birefringency of the two crystals, $\Phi_0(E_{Bias})$ and $\Phi_1(E_{Ext})$ describe the electro-optic properties of, respectively, the bias and sensing crystals which vary linearly with the applied electric field.

Eq. (1) constitutes the basis of the developed analytical model which supported selection of optical components for the proof-of-concept test bench. The model, developed in MATLAB, mimics the behaviour of the optical chain and accurately factors in effects related to temperature, optical wavelength and the level of doping of the crystals. It provides all the simulations results shown in the paper.

With no external field acting on the sensing crystal and with $E_{Mod} = 0$ on the bias crystal, the sensor's output light intensity depends only on E_{Bias} and is characterized by a quadratic transfer function shown in Fig. 2. The electric field equivalent to a half-period shift of the transfer function is called E_π and its value is given by:

$$E_\pi = \frac{\lambda}{L_y(n_e^3 r_{33} - n_o^3 r_{13})} \quad (2)$$

E_π corresponds to the electric field necessary to rotate the laser beam's polarisation by 180°. Each of the two crystals features its own E_π which are distinguished as $E_{\pi B}$ for the bias crystal and $E_{\pi S}$ for the sensing crystal. $E_{\pi B}$ limits the maximum useful modulation amplitude [11], whiles $E_{\pi S}$ defines, together with the acquisition chain, the resolution and the dynamic range of the optical chain.

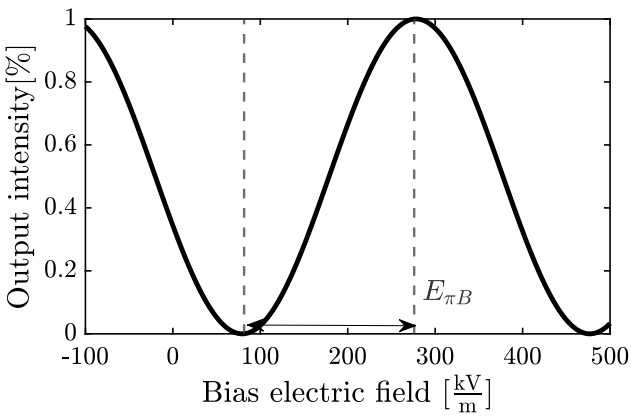

Figure 2: Transfer function of the modelled optical chain.

DC Field Measurements in Frequency Domain

The quadratic symmetry of the sensor's transfer function can be exploited to conduct DC measurements in the frequency domain. Firstly, in the absence of E_{Ext}, the DC bias is set to drive the system to one of the symmetry points (any peak or trough of the transfer function). A pure sinusoidal modulation applied around a symmetry point results in an output signal containing only even harmonics of the modulation frequency. Figure 3 shows the working point set with E_{Bias} (red dot) and the sinusoidal modulation E_{Mod} added on top (red line). The sinusoidal signal moves the working point along the transfer function, resulting in a modulated output signal containing exclusively even harmonics of the modulation frequency as shown in Fig. 4.

A DC particle beam, and its corresponding electrostatic field, acting on the sensing crystal, disrupts this symmetry by effectively shifting the working point by an amount proportional to the intensity of the measured field, as shown in Fig. 5. The resulting output signal, shown in the frequency domain in Fig. 6, contains both odd and even harmonics of the modulation frequency. Amplitudes of the odd harmonic are proportional to E_{Mod} and can therefore be used

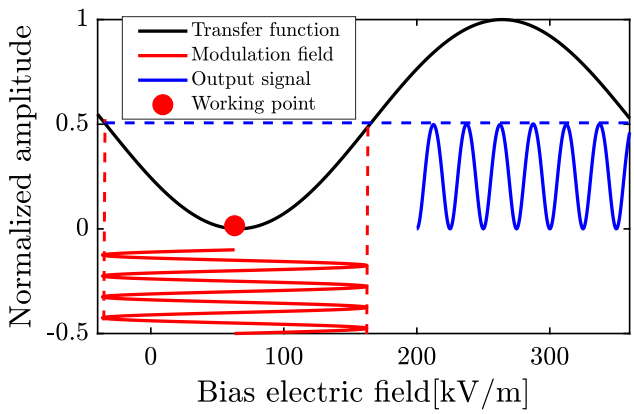

Figure 3: Output light intensity with a sinusoidal modulation applied to the bias crystal in standard condition, without electric field acting on the sensing crystal.

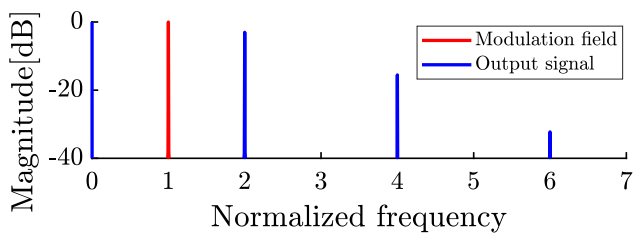

Figure 4: Spectrum of the modulation field and the modulated output intensity with no electric field acting on the sensing crystal.

ISBN: 978-3-95450-241-7 ISSN: 2673-5350 doi:10.18429/JACoW-IBIC2022-WEP10

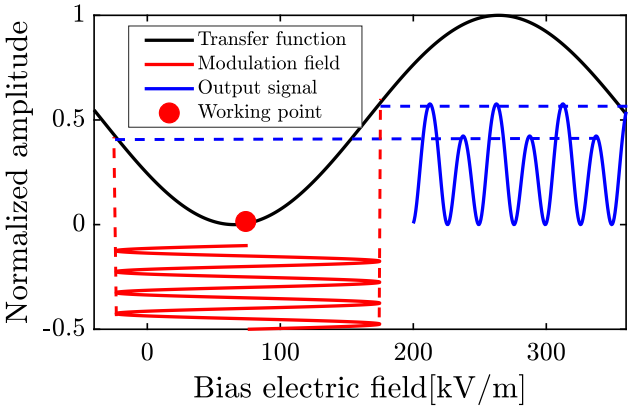

Figure 5: Output light intensity with a sinusoidal modulation applied to the bias crystal when an electric field is acting on the sensing crystal.

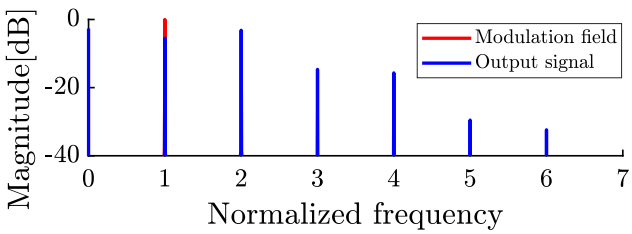

Figure 6: Spectrum of the modulation field and the modulated output intensity with an electric field acting on the sensing crystal.

to determine the relative intensity of the field under measurement [11]. Since for beam position monitoring the EO-DC-BPM does not require measurements of the absolute DC field intensity, there is no need to precisely calibrate the absolute electric field sensitivity of the sensor. Moreover, as the amplitude of the first harmonic is the strongest, the EO-DC-BPM fully relies on monitoring that component only.

EXPERIMENTAL RESULTS

The analytical model was validated experimentally with a proof-of-concept laboratory test bench shown in Fig. 7.

The test bench consists of a 60 cm long pipe with a square 45×45 mm aperture. Both vertical walls of the pipe carry removable crystal holders, annotated with a red circle in Fig. 7. The holder houses the sensing crystal and two prisms to steer the laser beam in and out of the pipe and through the crystal. The bias crystal is placed outside the pipe, between two PCBs connected to a high-voltage piezo-amplifier. The most relevant properties of the crystals are listed in Table 1.

The entire optical chain, except for the two crystals, was assembled using off-the-shelf THORLABS components. The SFL-1550P laser diode provides a 1550 nm linearly-polarised laser beam with a maximum power of 40 mW. The choice of the wavelength might seem counter-intuitive considering the figure of merit E_π defined earlier in Eq. (2). However, the selected wavelength minimizes the creation of optically induced hole-electron pairs which would otherwise be a source of unwanted space charge. The output laser beam is captured by the S122C photo-detector connected to the PM100D power meter, whose output is measured by a 10-bit oscilloscope and a signal analyzer.

A metal rod carrying a voltage up to 1 kV traverses the pipe longitudinally. The rod substitutes a DC particle beam passing through the EO-DC-BPM and acts as source of a uniform electric field for the sensing crystal. The pipe and the optical chain are fixed on a breadboard which, in turn, is mounted on a linear translation stage connected to a large optical table. The metallic rod is rigidly attached to the same optical table. Such a configuration allows the pipe and all the optics to be displaced around a stationary rod.

Table 1: Properties of the $LiNbO_3$ (5% MgO doped) Crystals Used in the EO Sensor

	Bias crystal	Sensing Crystal
$\mathbf{L_x}$ [mm]	3	5
$\mathbf{L_y}$ [mm]	40	50
$\mathbf{L_z}$ [mm]	3	2
$\mathbf{E}_\pi$ [$\frac{\mathrm{kV}}{\mathrm{m}}$]	$E_{\pi B}$ = 203.9	$E_{\pi S}$ =159

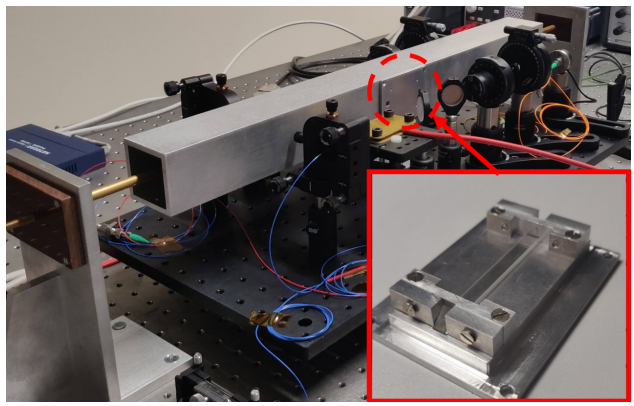

Figure 7: Proof-of-concept test bench and metallic holder highlighted.

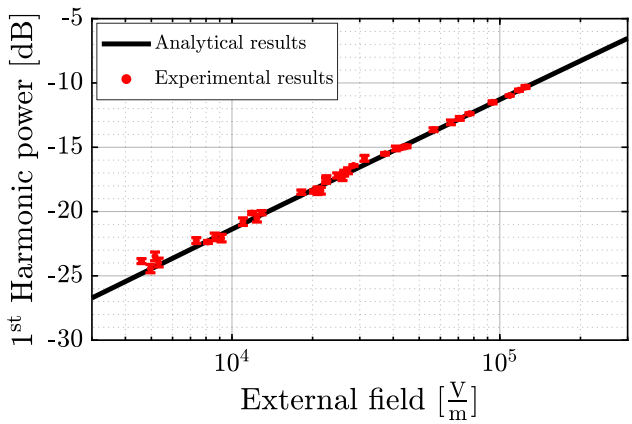

Figure 8: Experimental results of a single optical chain benchmarked with analytical ones.

Content from this work may be used under the terms of the CC BY 4.0 licence (© 2022). Any distribution of this work must maintain attribution to the author(s), title of the work, publisher, and DOI

ISBN: 978-3-95450-241-7 ISSN: 2673-5350 doi:10.18429/JACoW-IBIC2022-WEP10

Content from this work may be used under the terms of the CC BY 4.0 licence (© 2022). Any distribution of this work must maintain attribution to the author(s), title of the work, publisher, and DOI

Figure 8 shows the comparison of experimental results and analytical predictions. Data were sampled at f_s = 100 kSps while the biasing crystal was modulated at f_{Mod} = 600 Hz. The sensor measured an electric field ranging from 3 to 150 kV/m, and was limited on the lower end by the dynamic range of the used acquisition system. The maximum field was limited by the highest voltage which could be applied to the rod. Experimental observations show small discrepancies for low values of the electric field, which can be explained by several imperfections of this first proof-of-concept test bench such as space charge build-up, presence of higher harmonics in the modulation signal or uncompensated temperature drift. To better understand the reasons behind the discrepancies, a custom acquisition chain is under development to extend the dynamic range of the system. Additionally, the new acquisition chain will make it possible to simultaneously use a second optical branch installed on the opposite side of the pipe. Combining the information from the two optical chains, it will be possible to directly measure the position of the metallic rod inside the pipe.

Analytical Transverse Position Evaluation

The successful validation of the analytical model with experimental results makes estimating the transverse position resolution for an EO-DC-BPM using two symmetric optical branches possible. Table 2 summarizes the obtained results.

Table 2: Estimated transverse position measurement resolution. R* is the vacuum chamber aperture.

DAQ	I_b [A]	BW [Hz]	R* [mm]	DR [dB]	Position resolution [µm]
scope	2.8	59	45	30	3e3
custom	2.8	100	45	75	0.1
custom	0.28	100	45	75	1
custom	0.28	100	80	75	2.5

The first row gives the resolution estimate for the laboratory test bench with the same basic acquisition chain as used to obtain the experimental results presented in the previous section. The assumed beam current of 2.8 A is exactly one order of magnitude higher than the current of an unbunched beam in the SPS. The very modest 30 dB of dynamic range limits the minimum detectable displacement to 3 mm in a measurement bandwidth of 59 Hz.

The system performance can be significantly improved with a dedicated acquisition system, the development of which is currently ongoing. The new electronics will be based on the VFC acquisition card [13] together with a 24-bit ADC/DAC module, both developed at CERN. Moreover, the signal will be preconditioned with an analog circuit to isolate and amplify the first harmonic. The new system will replace the optical power meter and the 10-bit oscilloscope used to gather the first experimental data, which will lead to an effective improvement of the dynamic range by approximately 60 dB for a measurement bandwidth BW of 100 Hz. With a conservative margin of 15 dB for unknown sources of noise and nonlinearities, a dynamic range of 75 dB is deemed achievable with the new electronics. The second and third rows of Table 2 show the estimates for the developed test bench equipped with the improved acquisition system and measurement bandwidth increased to 100 Hz. The transverse position resolution decreases to less than 1 µm for the conditions of the previously discussed experiments.

The final row gives an estimate for a debunched SPS beam in a vacuum chamber with a realistic diameter of 80mm. The electric field in the crystal was computed for an improved design of the sensing crystal's holder (see Fig. 7), with no metal stripes partially covering the crystal. This leads to a 30% increase in the intensity of the electric field acting on the sensing crystal. Under these conditions, the computed resolution is 2.5 µm.

CONCLUSION

We have presented a conceptual design of a novel BPM composed of four identical EO electrostatic field sensors and capable of performing measurements of DC particle beams in the frequency domain.

The good match between the theoretical predictions of the analytical model and experimental results obtained on a purpose-built test bench confirms the feasibility of constructing such a sensor. The measurements can be applied over a wide range of electrostatic fields by varying the optical properties of the system.

Further improvements are being investigated. In particular, a custom acquisition system is under development not only to increase the resolution of the final system but also to open the possibility of studying the impact of parasitic effects of the EO crystals on the measurement's accuracy.

ACKNOWLEDGEMENTS

The authors express their gratitude to Juan Carlos Allica Santamaria, Franck Guy Guillot-Vignot, Patrick Bouvier, Morad Hamani, Thibaut Lefevre, Stefano Mazzoni, and Romain Ruffieux from the Beam Instrumentation Group at CERN, and Alberto Arteche from Royal Holloway University of London, for their help with the design and construction of the EO test bench and for the commissioning of the laser-lab. This project has received funding from the ATTRACT project funded by the EC under Grant Agreement 777222.

REFERENCES

[1] V. Kain, "Fixed Target Beams", CERN Proceedings 2, 2017.

[2] M. Anelli *et al.*, "A facility to search for hidden particles (SHiP) at the CERN SPS", arXiv preprint, 2015. doi:10.48550/arXiv.1504.04956

[3] S. Paret *et al.*, "Transverse Schottky and beam transfer function measurements in space charge affected coasting ion beams", *Phys. Rev. Spec. Top. Accel Beams*, vol. 13, no. 2,

ISBN: 978-3-95450-241-7 ISSN: 2673-5350 doi:10.18429/JACoW-IBIC2022-WEP10

p. 022802, 2010. doi:10.1103/PhysRevSTAB.13.022802

[4] R. Jung *et al.*, "Single pass optical profile monitoring", in *Proc. DIPAC 2003*, Mainz, Germany, May 2003, pp. 10-14.

[5] C. D. West and R. Clark Jones, "On the properties of polarisation elements as used in optical instruments. I. Fundamental considerations", *J. Opt. Soc. Am.*, vol. 41, no. 12, Dec. 1951, pp. 976-982. doi:10.1364/JOSA.41.000976

[6] A. Arteche, "Studies of a prototype of an electro-optic beam position monitor at the CERN super proton synchrotron", Ph.D. thesis, Royal Holloway, University of London, 2018.

[7] N. Kuwabara *et al.*, "Development and analysis of electric field sensor using LiNbO3 optical modulator", *IEEE Trans. Electromagn. Compat.*, vol 34, no. 4, Nov. 1992, pp. 391-396. doi:10.1109/15.179271

[8] J. Liu, H. Wang and Y. Li, "Research and design of rotary optical electric field sensor", in *IOP Conference Series: Materials Science and Engineering*, vol. 677, no. 5, Dec. 2019, p. 052112. doi:10.1088/1757-899x/677/5/052112

[9] R. S. Weis and T. K. Gaylord, "Lithium niobate: Summary of physical properties and crystal structure", *Appl. Phys.*, vol. 37, no. 4, Aug. 1985, pp. 191-203. doi:10.1007/BF00614817

[10] M. N. Palatnikov *et al.*, "Radiation hardness of lithium niobate nonlinear optical crystals doped with Y, Gd, and Mg", *Inorg. Mater.*, vol. 49, no. 8, Aug. 2013, pp. 821-825. doi:10.1134/S0020168513080116

[11] A. Cristiano, M. Krupa and R. Hill, "Electro-optic sensor for measuring electrostatic fields in the frequency domain", *Appl. Sci.-Basel*, vol. 12, no. 17, Sep. 2022, p. 8544. doi:10.3390/app12178544

[12] R. Clark Jones, "A new calculus for the treatment of optical systemsi. description and discussion of the calculus", *J. Opt. Soc. Am.*, vol. 31, no. 7, Jul. 1941, pp. 488-493. doi:10.1364/JOSA.31.000488

[13] A Boccardi *et al.*, "A modular approach to acquisition systems for future CERN beam instrumentation developments", in *Proc. ICALEPS'15*, Melbourne, Australia, Oct. 2015. pp. 1103–1106. doi:10.18429/JACoW-ICALEPCS2015-THHB2O02

Content from this work may be used under the terms of the CC BY 4.0 licence (© 2022). Any distribution of this work must maintain attribution to the author(s), title of the work, publisher, and DOI